Proceedings of the
International Conference on Mechanical Engineering 2011
(ICME2011) 18-20 December 2011, Dhaka, Bangladesh

ICME11-FL-023

MODELLING OF GAS-LIQUID BUBBLY FLOWS IN PRACTICAL VERTICAL PIPES

Jiyuan Tu[1], L. Deju[1], Sherman CP Cheung[1], Guan H. Yeoh[2], E. Krepper[3] and D Lucas[3]

[1]School of Aerospace, Mechanical and Manufacturing Engineering, RMIT University, Australia.
[2]Australian Nuclear Science and Technology Organization (ANSTO), NSW 2234, Australia.
[3]Institute of Safety Research, Forschungszentrum Rossendrof e.V., 01314 Dresden, Germany.

ABSTRACT

In many multiphase flow systems, gas-liquid bubbly flows (i.e. swarm of discrete gas bubbles suspended in continuous liquid) have a wide range of applications; including mining, pharmaceutical and petroleum industries. To enhance the efficiency of their systems, large interfacial area between bubbles and liquid is of foremost importance to facilitate gas-liquid reactions (oxidation, hydrogenation, halogenations, aerobic fermentation, etc.). Accurate prediction of the phase distribution and interaction via computational schemes poses a great potential to optimize existing systems. The implementation of Population Balance (PB) in Computational Fluid Dynamics (CFD) is an important emerging approach in solving such complex bubbly flows. Nonetheless, in general, current PB models are computationally expensive and simulations for practical system require intractable CPU time. In order to address this issue, a promising alternative PB model –direct quadrature method of moments (DQMOM) is presented and assessed for handling practical bubbly flows. In contrast to MUSIG model that requires large number of classes to resolve the bubble distribution, the main advantage of DQMOM is that the number of moments to be solved is generally very small. To assess the performances of DQMOM model – in tracking the changes of gas volume fraction and bubble size distribution under complex flow conditions, numerical studies have been carried out to validate predictions against experimental data of Lucas et al. [1] and Prasser et al. [2] measured in the Forschungszentrum Dresden-Rossendorf FZD facility. Preliminary results have been found to compare reasonably well against experimental data as well as the widely adopted PB model (i.e. MUSIG) predictions. Good agreement between the predictions and experimental measurements demonstrates that the computational efficiency for DQMOM could adequately capture the wide bubble size range prevalent in large pipe flows in comparison to the use of MUSIG model which requires substantial computational resources.

Keywords: Population Balance, Bubbly Flow, DQMOM

1. INTRODUCTION

There are many industrial processes that involve gas-liquid dispersion in stirred tanks, for example in fine-chemical manufacturing or in biochemical fermentations. For economic, as well as safety reasons, it is necessary to develop good models for designing of such reactors. The ability to predict the void fraction distribution and understanding of the physical mechanisms determining bubble size is crucial to any detailed theory of the transfer of heat, mass and momentum between phases and also provides essential information toward assessments of safer reactor designs and operations. Relevant experimental observations have revealed clear tendencies of the bubbles within the bulk liquid flow to undergo deformation, coalescence, breakage and condensation within the particular system of interest subject to local flow conditions and heat and mass transfer processes. Nevertheless, from a modelling perspective, enormous challenges remain in fully resolving the many associated interfacial effects occurring between different phases subject to turbulence for a wide range of gas–liquid bubbly flows.

Bubble size distribution in vertical pipes is not constant; rather it may change due to bubble-bubble interactions due to breakage or coalescence. No broadly applicable model for the determination of bubble size has yet been presented due to the insufficient understanding of the physical mechanisms. The presence of turbulence of the liquid phase especially in large scale industrial two-phase system will cause the larger bubbles to break-up until a dynamic equilibrium is reached. While disperse bubbly flows with low gas volume fractions are mostly mono-disperse, an increase of the gas volume leads to a broader bubble size distribution where bubbles

are subject to migration due to non-drag forces acting in lateral direction. These lateral bubble forces as well as the drag and the virtual mass force depend on the bubble size [3]. Especially for the lift force was found to change its direction as the bubble size varies [4, 5].

An adequate modelling approach has to account for all these phenomena. Since the interfacial area concentration represents the key parameter that links the interaction between phases, much attention have been concentrated towards better understanding the coalescence and breakage of bubbles and between bubbles and turbulent eddies. From the early introduction to commercial package [6], the population balance approach based on the MUSIG model has been frequently employed to predict the non-uniform bubble size distribution in a gas-liquid mixture by solving a range of bubble classes. Although encouraging results have been reported [7, 8], flows in large pipe with large bubble diameter, computational resource for solving such large number of transport equations could be extremely excessive. In this paper, DQMOM approach has been presented by the consideration of Method of Moments (MOM). Here, the bubble size distribution is tracked through its moments by integrating out the internal coordinates. Prediction by the DQMOM and MUSIG models are validated against gas-liquid flow experiments in vertical pipes of medium size by Lucas, Krepper et al. [1] and large size of Prasser, Beyer et al. [2] measured in the Forschungszentrum Dresden-Rossendorf FZD facility.

2. MODEL DESCRIPTION

2.1 Two fluid model for gas-liquid flow

The two-fluid model treating both the gas and liquid phases as continua solves two sets of conservation equations governing mass and momentum. Denoting the liquid as the continuum phase (α_l) and the gas (i.e. bubbles) as disperse phase (α_g), these equations can be written as:

$$\frac{\partial}{\partial t}\left(\rho_i \alpha_i\right) + \nabla.\left(\rho_i \alpha_i \bar{u}_i\right) = 0 \tag{1}$$

$$\begin{aligned} &\frac{\partial}{\partial t}\left(\rho_i \alpha_i \bar{u}_i\right) + \nabla.\left(\rho_i \alpha_i \bar{u}_i \bar{u}_i\right) = \\ &-\alpha_i \nabla P + \alpha_i \rho_i \bar{g} + \nabla.\left[\alpha_i \mu_i^e \left(\nabla \bar{u}_i + \left(\nabla \bar{u}_i\right)^T\right)\right] + F_i \end{aligned} \tag{2}$$

where $\bar{g}$ the gravity acceleration vector and P is the pressure. The closure law is required to determine the momentum transfer of the total interfacial force. This force strongly governs the distribution of the liquid and gas phases within the flow volume. On the right hand side of equation (2), F_i represents the total interfacial force which is composed of the drag force, lift force, wall lubrication force and the turbulent dispersion force respectively. Numerical details on handling these interfacial forces can be found in [9] and references therein. For handling the turbulence effects, the Shear Stress Transport (SST) model is adopted for the liquid phase [10], while the Sato's bubble-induced turbulent viscosity model [11] was employed for the gas phase.

2.2 MUltiple SIze Group (MUSIG) Model

In accordance with Fleischer, Becker et al. [12], the bubble size distribution is calculated with population balance equation (PBE) that is generally expressed in an integro-differential form describing the local Bubble Size Distribution (BSD) written as

$$\frac{\partial f\left(x,\xi,t\right)}{\partial t} + \nabla.\left(V\left(x,\xi,t\right) f\left(x,\xi,t\right)\right) = S\left(x,\xi,t\right) \tag{3}$$

where $f\left(x,\xi,t\right)$ is the bubble number density distribution per unit mixture and bubble volume, $V\left(x,\xi,t\right)$ is velocity vector. On the right hand side, the term $S\left(x,\xi,t\right)$ contains the bubble source/sink rates per unit mixture volume due to the bubble interactions such as coalescence, break-up and phase change.

Table 1: Flow conditions of all test cases and its inlet boundary conditions

MTLOOP Experiment			
		Case M107	**Case M118**
$[\langle j_l \rangle\|_{Z/D=0}]$	(m/s)	**1.017**	**1.017**
$[\langle j_l \rangle\|_{Z/D=0}]$	(m/s)	**0.140**	**0.219**
$[\alpha_g\|_{Z/D=0}]$	(%)	**[12.1]**	**[17.72]**
$[D_S\|_{z/D=0.0}]$	(mm)	**[5.14]**	**[6.38]**
TOPFLOW Experiment			
		Case T107	**Case T118**
$[\langle j_l \rangle\|_{Z/D=0}]$	(m/s)	**1.017**	**1.017**
$[\langle j_l \rangle\|_{Z/D=0}]$	(m/s)	**0.140**	**0.2194**
$[\alpha_g\|_{Z/D=0}]$	(%)	**[12.1]**	**[17.72]**
$[D_S\|_{z/D=0.0}]$	(mm)	**[20.18]**	**[23.28]**

A sophisticated model, namely MUltiple SIze Group (MUSIG) was first introduced by Lo [6] and is today the most commonly used technique for solving PBE. The technique proposed by Kumar and Ramkrishna [13] that allows the usage of variable M bubble size groups to reduce the numerical effort is adopted, such as:

$$\frac{\partial n_i}{\partial t} + \nabla.\left(u_i^g n_i\right) = S_i \tag{4}$$

The interaction term $S_i = \left(P^C + P^B - D^C - D^B\right)$ contains the source rates of P^C, P^B, D^C and D^B, which are the production rates due to coalescence and break-up and the death rate to coalescence and break-up of bubbles respectively. The birth and death rates can be formulated in terms of size fraction.

$$P^C = \left(\rho_j^g \alpha_j^g\right)^2 \frac{1}{2} \sum_k \sum_l f_k f_l \frac{M_k + M_l}{M_k M_l} a\left(M_k, M_l\right) \quad (5)$$

$$D^C = \left(\rho_j^g \alpha_j^g\right)^2 \sum_k f_i f_k \frac{1}{M_k} a\left(M_i, M_k\right) \quad (6)$$

$$P^B = \rho_j^g \alpha_j^g \sum_k r\left(M_k, M_i\right) f_k \quad (7)$$

$$D^B = \rho_j^g \alpha_j^g f_i \sum_k r\left(M_i, M_k\right) \quad (8)$$

2.3 Direct quadrature method of moments (DQMOM)

The DQMOM is based on the direct solution of the transport equations for weights and abscissas of the quadrature approximation [14]. According to Marchisio and Fox [15] the main idea is to keep track the primitive variables appearing in the quadrature approximation, instead of moments of the BSD.

The weights and abscissas can be related to the size fraction of the dispersed phase (f_k) and a variable defined as $\psi_k = f_k / M_k$. The size fraction of f_k is related to the weights and abscissas by:

$$\rho_g \alpha_g f_k = N_i M_i = \zeta_k \quad (9)$$

Using the above expression, the transport equations become:

$$\frac{\partial\left(\rho_g \alpha_g f_k\right)}{\partial t} + \nabla.\left(\rho_g \alpha_g \bar{u}_g f_k\right) = b \quad (10)$$

$$\frac{\partial\left(\rho_g \alpha_g \psi_k\right)}{\partial t} + \nabla.\left(\rho_g \alpha_g \bar{u}_g \psi_k\right) = a \quad (11)$$

The moment transform of the coalescence and break-up of the term S_k can then be expressed as:

$$S_k = \left(P_k^C - D_k^C + P_k^B - D_k^B\right) \quad (12)$$

Where the terms P and D represent the birth and death rates of the coalescence and break-up of bubbles which is equivalent to $S\left(x, \xi, t\right)$ in equation (3).

Coalescence kernel by Prince and Blanch [16] and break-up mechanism of Luo and Svendsen [17] were employed to evaluate the above birth and death rates.

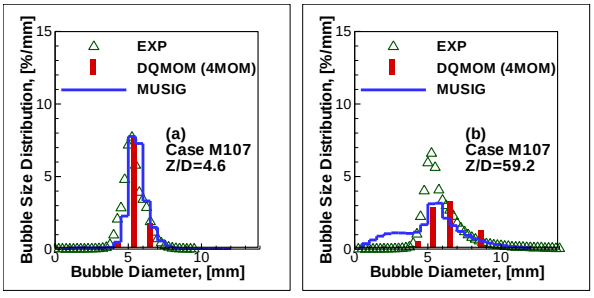

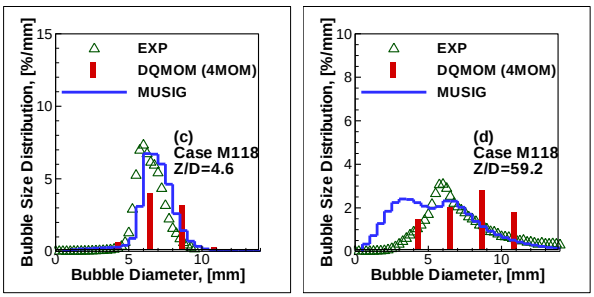

Fig 1. Comparison of predicted bubble size distribution for MTLOOP

3. EXPERIMENTAL DETAILS

Two individual set of experiments – MTLOOP [1] and TOPFLOW [2]– that have been performed in the Forschungszentrum Dresden-Rossendorf FZD facility was considered for the validation of simulation results. Experimental details on flow measurement and setup can be found out from [1] and [2].

4.NUMERICAL DETAILS AND RESULTS

Numerical calculations were achieved through the use of the generic computational fluid dynamics code ANSYS-CFX11 [19]. The DQMOM transport equation with appropriate source and sink terms describing the coalescence and break-up rate of bubble was implemented through the CFX Command Language (CCL).

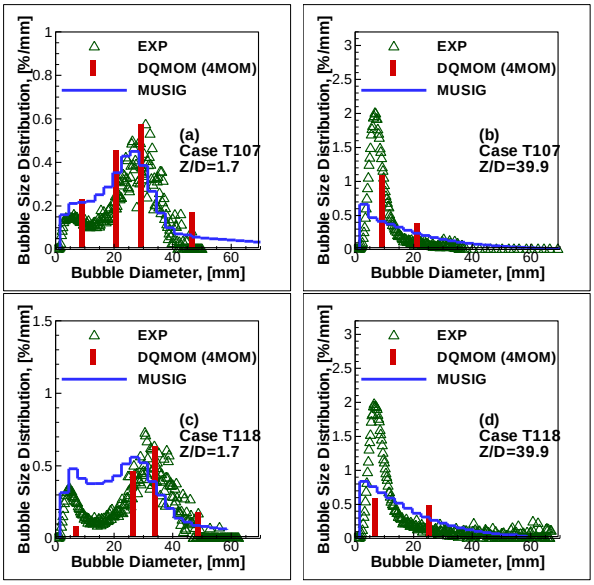

Fig 2. Comparison of predicted bubble size distribution for TOPFLOW

Radial symmetry was assumed in both experimental conditions thereby allowing the computational geometry to be simplified through consideration of a 60° radial sector of the pipe with symmetry boundary conditions being imposed at both vertical sides of the computational domain. Four sets of experiment data under two different flow conditions – hereafter denoted as case M107, M118, T107 and T118 – were selected from both experiments. For the MTLOOP experiment, a uniform gas volume

fraction was specified at the inlet boundary. On the other hand, 12 equally spaced point sources of the gas phase were placed at the circumference of the 60^0 radial sectors to represent the wall injection method in TOPFLOW. Gas injection rate at each point source was assumed to be identical. Details of the boundary conditions are summarized in Table 1. Based on grid sensitivity test performed for the MTLOOP and TOPFLOW experiments, grid independent solutions have revealed that computational meshes which consisted of 18,223 elements for MTLOOP and 48,000 elements for TOPFLOW did not appreciably change even though finer computational meshes were tested. For all flow conditions, reliable convergence criterion based on RMS (root mean square) residual of 1.0×10^{-4} was adopted for the termination of numerical calculations.

Following the study carried out by Krepper, Lucas et al. [18], dimensionless factors for the mass transfer rates of breakage F_B = 0.25 and F_C = 0.05 for the coalescence were adapted to harmonize the mechanism of bubble coalescence and break-up kernels of the MUSIG and DQMOM model. For comparison purpose, these dimensionless factors were kept constant for all test cases in during the entire numerical calculations.

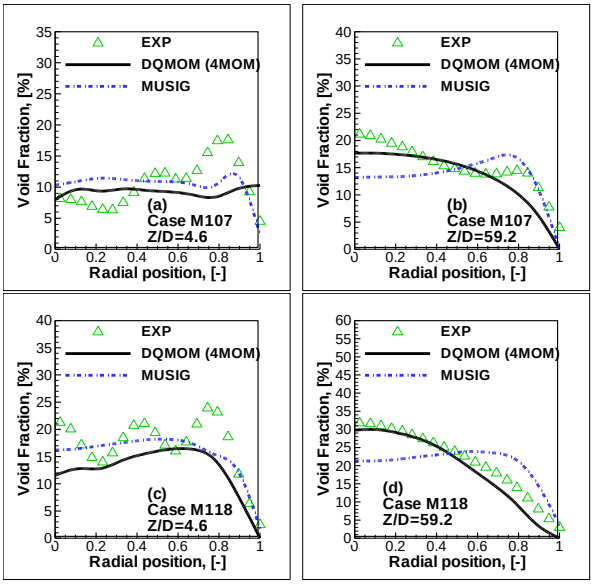

Fig 3. Comparison of the predicted radial gas volume fraction distributions for MTLOOP

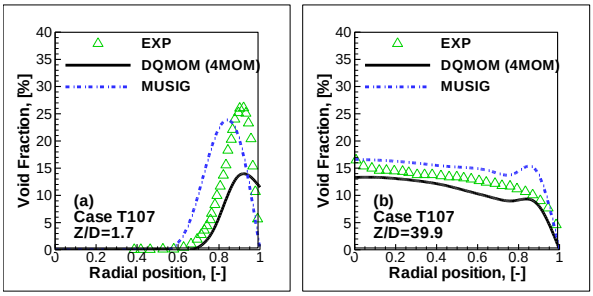

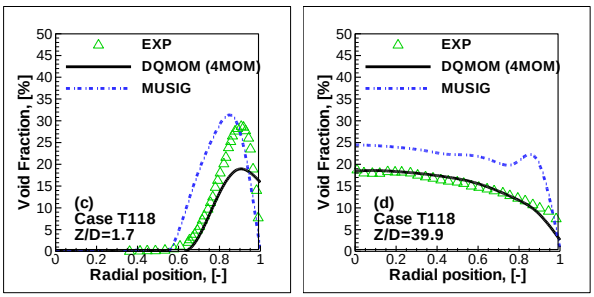

Fig 4. Comparison of the predicted radial gas volume fraction distributions for TOPFLOW

4.1 Change in Bubble size distribution due to Coalescence and Breakage

Fig 1 shows the predicted cross- sectional averaged bubble size distribution from the DQMOM model with 4 moments in comparison with the MTLOOP experimental data. The axial development of the measured area averaged Sauter mean diameter was assessed and predictions were compared at the measuring stations of z/D = 4.5 and 60. In order to assess its predictive capability, additional comparison is also carried out against the predicted MUSIG results. Close to the gas injection capillaries where coalescence processes began, the initial bubble size distributions were considerably narrow. However, as shown in Fig 1b &1d, the bubble size distribution has significantly widened after a series of merging procedures.

It has emerged that the MUSIG model has over predicted the small bubbles at the axial location of z/D = 60. This could possibly due to homogeneous MUSIG model application. In general, prediction from the DQMOM model was reasonably well agreed with the measurement for TOPFLOW experiment at different axial location of z/D = 1.7 and 39.9. According to Fig 2, bimodal peak was found close to the vicinity of injection unit for both the models. For well developed flow bubble size distribution was relatively narrower and single-peaked profile in well agreement with the experiment.

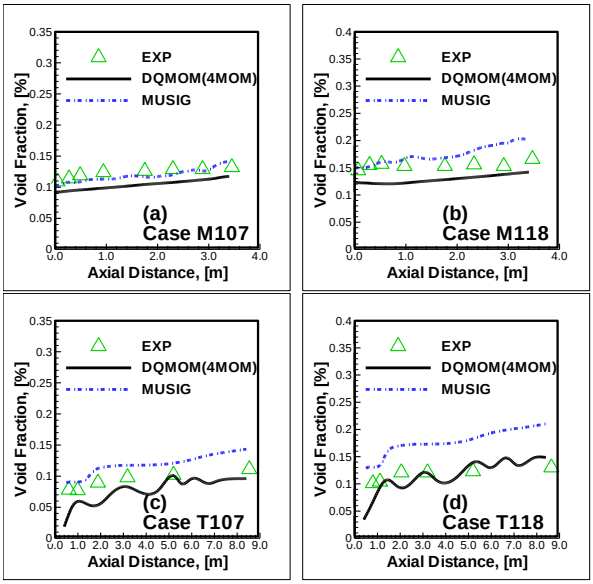

Fig 5. Comparison of the predicted axial gas volume fraction distributions

4.2 Void fraction distribution

The behavior of void fraction profiles measured at z/D=4.5 and 60 in MTLOOP experiment for different flow condition of M107 and M118 is depicted in Fig 3. As can be seen various phase distribution patterns were observed in the present experiment, and void fraction profiles from DQMOM and MUSIG model were found to be capable of successfully predicted the separation between small and large bubbles within the gas-liquid flows. For both flow condition of M107 and M118 of DQMOM and MUSIG model, the void fraction radial profile evolves from a wall-peak to a core-peak trend all the way through radial direction. This clearly demonstrates that the adopted interfacial force models successfully predicted the trend of the gas phase lateral motions and the evolution of smaller bubbles to larger bubbles shows the dominant effect of bubble coalescence. It appeared that DQMOM gave slightly better predictions especially at the well-developed core peaking characteristics at z/D = 60 in both test cases of M107 and M118. However, as depicted from Fig 3b & 3d void fraction at the core of the pipe slightly under predicted by MUSIG model. The possible explanation of the under-prediction could be caused by the uncertainties concerning the turbulence model which predicted the turbulent energy dissipation and coupled with the coalescence and breakage model.

For TOPFLOW experiment Fig 4 shows the void fraction distribution obtained from the DQMOM model comparing with the MUSIG model and measured data at the dimensionless axial position z/D = 1.7 and 39.9. Both models were capable to capture the transition process from 'wall peak' to 'core peak' of the gas volume fraction profile. Unlike the behavior of the MTLOOP the bubbles were injected from the gas injection orifices located on the circumference of the pipe, highly concentrated bubbles were formed within the wall proximity that results 'wall peak' void fraction distribution close to inlet of the pipe. Predicted gas volume fraction profile for both models in axial direction is also in good agreement with the measurement as illustrated in Fig 5. Due to pressure gradient the bubble expansion occurs therefore average void fraction increases over the axial distance. Thus DQMOM model capability is validated for modelling gas-liquid flow with rigorous bubble interactions.

Table.2: Computational Time

	Time
MUSIG - MTLOOP 118 (20 Size group)	53hrs
DQMOM - MTLOOP 118 (4MOM)	3 hrs
MUSIG – TOPFLOW 118 (20 Size group)	82 hrs
DQMOM - MTLOOP 118 (4MOM)	14 hrs

5. CONCLUSION

The assessment of two population balance models – MUSIG and DQMOM models – has been performed against the experimental data of Lucas et al. [1] and Prasser et al. [2] measured in Forschungszentrum Dresden-Rossendorf FZD facility. With two different gas injection methods, bubble coalescence was found to be dominant feature in the MTLOOP experiment while bubble break-up prevailed as the main characteristics in the TOPFLOW experiment. Owing to the high resolution of bubble sizes that can be achieved via the use of the MUSIG model, encouraging results have been attained. Nonetheless, the MUSIG model required to solve extra transport equations posing significant burden to both computational time and resources as depicted in Table. 2. Although very few number of scalars were necessary to solve for DQMOM, encouraging results clearly demonstrated that the evolution of bubble sizes was well captured by the DQMOM model. With the relatively compact mathematical expression, the DQMOM model can be considered as an efficient and attractive alternative for population balance modeling of gas-liquid flows.

6. REFERENCES

1. Lucas, D., E. Krepper, and H.M. Prasser, Development of co-current air-water flow in a vertical pipe. International Journal of Multiphase Flow, 2005. **31**(12): p. 1304-1328.
2. Prasser, H.M., et al., Evolution of the structure of a gas-liquid two-phase flow in a large vertical pipe. Nuclear Engineering and Design, 2007. **237**(15-17): p. 1848-1861.
3. Lucas, D., E. Krepper, and H.M. Prasser, Use of models for lift, wall and turbulent dispersion forces acting on bubbles for poly-disperse flows. Chemical Engineering Science, 2007. **62**(15): p. 4146-4157.
4. Bothe, D., M. Schmidtke, and H.J. Warnecke, VOF-simulation of the lift force for single bubbles in a simple shear flow. Chemical Engineering & Technology, 2006. **29**(9): p. 1048-1053.
5. Tomiyama, A., Struggle with computational bubble dynamics, in *Third International Conference on Multiphase Flow*. 1998: Lyon, France 157.
6. Lo, S.M., Application of Population Balance to

CFD Modelling of Bubbly Flow via the MUSIG model. AEA Technology, AEAT-1096, 1996.
7. Chen, P., J. Sanyal, and M.P. Dudukovic, CFD modeling of bubble columns flows: implementation of population balance. Chemical Engineering Science, 2004. **59**: p. 5201-5207.
8. Duan, X.Y., et al., Gas-liquid flows in medium and large vertical pipes. Chemical Engineering Science, 2011. **66**(5): p. 872-883.
9. Cheung, S.C.P., G.H. Yeoh, and J.Y. Tu, On the modelling of population balance in isothermal vertical bubbly flows - Average bubble number density approach. Chemical Engineering and Processing, 2007. **46**(8): p. 742-756.
10. Menter, F.R., 2-Equation eddy-visocity turbulence models for engineering applications. Aiaa Journal, 1994. **32**(8): p. 1598-1605.
11. Sato, Y., M. Sadatomi, and K. Sekoguchi, Momentum and Heat-Transfer in 2-Phase Bubble Flow .1. Theory. International Journal of Multiphase Flow, 1981. **7**(2): p. 167-177.
12. Fleischer, C., S. Becker, and G. Eigenberger, Detailed modeling of the chemisorption of CO2 into NaOH in a bubble column. Chemical Engineering Science, 1996. **51**(10): p. 1715-1724.
13. Kumar, S. and D. Ramkrishna, On the solution of population balance equations by discrettization .1. A fixed pivot technique. Chemical Engineering Science, 1996. **51**(8): p. 1311-1332.
14. Fan, R., D.L. Marchisio, and R.O. Fox, Application of the direct quadrature method of moments to polydisperse gas-solid fluidized beds. Powder Technology, 2004. **139**(1): p. 7-20.
15. Marchisio, D.L. and R.O. Fox, Solution of population balance equations using the direct quadrature method of moments. Journal of Aerosol Science, 2005. **36**(1): p. 43-73.
16. Prince, M.J. and H.W. Blanch, Bubble Coalescence and Break-up in Air-Sparged Bubble-Columns. Aiche Journal, 1990. **36**(10): p. 1485-1499.
17. Luo, H. and H.F. Svendsen, Theoretical model for drop and bubble breakup in turbulent dispersions. Aiche Journal, 1996. **42**(5): p. 1225-1233.
18. Krepper, E., et al., The inhomogeneous MUSIG model for the simulation of polydispersed flows. Nuclear Engineering and Design, 2008. **238**(7): p. 1690-1702.
19. CFX-11, 2007. User Manual, ANSYS CFX.

7. NOMENCLATURE

Symbol	Meaning	Unit
D_s	Bubble Sauter Mean Diameter	(mm)
j	Superficial Velocity	(m/s)
P	Pressure	(Pa)
t	Bubble Contact Time	(s)
α	Void Fraction	(-)
ε	Turbulence Kinetic Energy Dissipation	(m^2/s^3)
ρ	Density	(kg/m^3)
σ	Surface Tension	(N/m)
μ^e	Effective Viscosity	(Pa.s)